Eur Biophys J (2009) 38:465–478
DOI 10.1007/s00249-008-0396-7

ORIGINAL PAPER

Movements of native C505 during channel gating in CNGA1 channels

Anil V. Nair · Claudio Anselmi · Monica Mazzolini

Received: 2 September 2008 / Revised: 9 December 2008 / Accepted: 11 December 2008 / Published online: 9 January 2009

Abstract We investigated conformational changes occurring in the C-linker and cyclic nucleotide-binding (CNB) domain of CNGA1 channels by analyzing the inhibition induced by thiol-specific reagents in mutant channels Q409C and A414C in the open and closed state. Cd^{2+} (200 μM) inhibited irreversibly mutant channels Q409C and A414C in the closed but not in the open state. Cd^{2+} inhibition was abolished in the mutant $A414C_{cys\text{-}free}$, in the double mutant A414C + C505T and in the tandem construct A414C + C505T/CNGA1, but it was present in the construct $A414C + C505_{cys\text{-}free}$. The cross-linker reagent M-2-M inhibited mutant channel Q409C in the open state. M-2-M inhibition in the open state was abolished in the double mutant Q409C + C505T and in the tandem construct Q409C + C505T/CNGA1. These results show that C_α of C505 in the closed state is located at a distance between 4 and 10.5 Å from the C_α of A414 of the same subunit, but in the open state C505 moves towards Q409 of the same subunit at a distance that ranges from 10.5 to 12.3 Å from C_α of this residue. These results are not consistent with a 3-D structure of the CNGA1 channel homologous to the structure of HCN2 channels either in the open or in the closed state.

Keywords Gating · Ionic channels · CNGA1 channels · Cd^{2+} inhibition · S6 domain

Abbreviations

CNG	Cyclic nucleotide-gated
CNBD	Cyclic nucleotide-binding domain
CSM	Cysteine scanning mutagenesis
MTS	Methanethiosulfonate
M-2-M	1,2-Ethanediyl bismethanethiosulfonate
M-4-M	1,4-Butanediyl bismethanethiosulfonate
DTT	Dithiothreitol

Introduction

Cyclic nucleotide-gated (CNG) channels underlie sensory transduction in vertebrate photoreceptors and in olfactory sensory neurons. These channels open when cyclic nucleotides such as cAMP or cGMP bind to a specific domain, usually referred to as the cyclic nucleotide-binding (CNB) domain (Fesenko et al. 1985; Zimmerman et al. 1985; Nakamura and Gold 1987; Kaupp et al. 1989; Zagotta and Siegelbaum 1996; Biel et al. 1999; Craven and Zagotta 2006; Kaupp and Seifert 2002). As opposed to the usual Na^+ and K^+ channels, CNG channels are cation selective, but poorly selective for monovalent alkali cations (Zimmerman and Baylor 1986; Kaupp et al. 1989; Menini 1990; Picco and Menini 1993; Craven and Zagotta 2006). They also form a tetrameric assembly of several homologous subunits (Chen et al. 1994; Körschen et al. 1995; Shammat and Gordon 1999; Zheng et al. 2002; Zhong et al. 2002;

A. V. Nair · C. Anselmi · M. Mazzolini (✉)
SISSA, International School for Advanced Studies, Neurobiology Sector, Area Science Park, Edificio Q1, SS 14 Km 163,5, 34012 Basovizza (TS), Italy
e-mail: mazzolin@sissa.it

C. Anselmi
SISSA and CNR-INFM-DEMOCRITOS Modeling Center for Research in Atomistic Simulation, Via Beirut 2-4, 34014 Trieste, Italy

Present Address:
A. V. Nair
Department of Physiology, Nijmegen Centre for Molecular Life Sciences, Radboud University, Nijmegen Medical Centre, P.O. Box 9101, 6500 HB Nijmegen, The Netherlands

Craven and Zagotta 2006), referred to as CNGA1-4 and CNGB1,3 (Bradley et al. 2001). The CNGA1 channel from bovine rods is composed of 690 residues, corresponding to about 80 kDa (Kaupp et al. 1989) and each subunit encodes for a CNB domain consisting of about 125 amino acids in the cytoplasmic C-terminal (Kaupp et al. 1989; Zagotta and Siegelbaum 1996). The CNB domain connects to the transmembrane domain of CNG channels through another domain composed of about 77 amino acids referred to as the C-linker.

The amino acid sequence of CNG and K^+ channels share a significant sequence similarity and both channels are members of the superfamily of voltage-gated channels (Zagotta and Siegelbaum 1996; Biel et al. 1999). They also have a significant sequence similarity with the family of hyperpolarization-activated and cyclic nucleotide-gated (HCN) channels (Anselmi et al. 2007), composed of four isoforms called HCN1–4 (Hofmann et al. 2005). All these channels open when the membrane potential is hyperpolarized and their activation properties can be modulated, to some extent, by cyclic nucleotides. The 3-D structure of murine HCN2 C-linker and of CNB domains has been recently solved (Zagotta et al. 2003): the sequence alignment of these domains in HCN2 and bovine CNGA1 channels indicates a sequence identity of 35%. This indicates that the overall folding of the C-linker domain of HCN2 and CNGA1 channels could be similar, and these domains in the two channels could have a common 3-D architecture.

The purpose of the present manuscript is to obtain experimental constraints on the relative distance between amino acids to test the hypothesis that the C-linker and CNB domains in CNGA1 and HCN2 channels share the same 3-D structure. Here we show that in the closed state C505 is close to A414 of the same subunit but in the open state it moves near Q409 of the same subunit. These results are not consistent with the 3-D structure of the CNGA1 channel, which is similar to the structure of HCN2 channels, either in the open or in the closed state.

Materials and methods

Molecular biology

Three different channel constructs from bovine rods were used: the CNGA1 channel (about 80 kDa), the tandem dimer construct (CNGA1/CNGA1, about 160 kDa) generated as previously described (Mazzolini et al. 2008), and the $CNGA1_{cys\text{-}free}$ channel (Matulef et al. 1999). Selected residues were replaced by introducing a cysteine in the three channels also as previously described (Becchetti et al. 1999; Matulef et al. 1999) using the Quick Change Site-Directed Mutagenesis kit (Stratagene). Point mutations were confirmed by sequencing, using the sequencer LI-COR (4000L). cDNAs were linearized and were transcribed to cRNA in vitro using the mMessage mMachine kit (Ambion, Austin, TX).

Mutant channels constructed inside the three different backgrounds are indicated in the following way: when residue X in position 999 is mutated in residue Y, in the CNGA1 background the mutant channel is indicated as X999Y (e.g., Q409C); in the $CNGA1_{cys\text{-}free}$ background, mutant channels are indicated similarly, but the subscript "cys-free" is added (for example $Q409C_{cys\text{-}free}$); the double mutations made in the same construct are indicated by adding a "plus" (+) symbol between the two mutations (e.g., Q409C + C505T or Q409C + $C505T_{cys\text{-}free}$); mutant channels in the tandem background are indicated by using the "slash" (/) symbol between the two different subunits linked together (e.g., Q409C + C505T/CNGA1).

Oocyte preparation and chemicals

Mutant channel cRNAs were injected into *Xenopus laevis* oocytes ("Xenopus express" Ancienne Ecole de Vernassal, Le Bourg 43270, Vernassal, Haute-Loire, France). Oocytes were prepared as previously described (Nizzari et al. 1993). Injected eggs were maintained at 19°C in a Barth solution supplemented with 50 μg/ml of gentamycin sulfate and containing (in mM): 88 NaCl, 1 KCl, 0.82 $MgSO_4$, 0.33 $Ca(NO_3)_2$, 0.41 $CaCl_2$, 2.4 $NaHCO_3$, 5 Tris–HCl (pH 7.4 buffered with NaOH). During the experiments, oocytes were kept in a Ringer solution containing (in mM): 110 NaCl, 2.5 KCl, 1 $CaCl_2$, 1.6 $MgCl_2$, 10 HEPES–NaOH (pH 7.4 buffered with NaOH). Usual salts and reagents were purchased from Sigma Chemicals (St Louis, MO, USA) and methanethiosulfonate (MTS) cross-linkers (1,2-ethanediyl bismethanethiosulfonate (M-2-M) and 1,4-butanediyl bismethanethiosulfonate (M-4-M)) were purchased from TRC (Toronto Research Chemicals, Canada).

Protein preparation and immunoblotting

After 4-day incubation at 19°C, batches of 15–20 oocytes were homogenized in 200 μL of homogenization buffer (100 mM Tris–HCl, 100 mM NaCl, 0.5% v/v Triton X-100, pH 8.0, supplemented with protease inhibitors) by trituration. The homogenate was incubated on ice for 15 min and then centrifuged at 16,000*g* for 10 min at 4°C. The soluble fraction was removed and placed into a clean tube, avoiding the pellet and the floating layer of the yolk, then centrifuged at 16,000*g* for 10 min. Then it was centrifuged one additional time at 16,000*g* for 10 min and transferred into a clean tube. About 50 min after homogenization, 20 mM *N*-ethylmaleimide (NEM, Sigma-Aldrich) was added in order to prevent further disulfide bond formation. A 20 μL of the

soluble fraction was then added to 10 µL loading dye (125 mM Tris–HCl, 6% v/v SDS, 20% v/v glycerol, 10% v/v bromophenol blue, pH 6.8) in the absence or in the presence of 10% v/v β-mercaptoethanol (β-ME) (Sigma-Aldrich) or 100 mM DTT (Sigma-Aldrich). Samples were subjected to SDS-PAGE using 3–8% acrilamide gel. After SDS-PAGE, proteins were transferred to a nitrocellulose filter by electroblotting. After the transfer, channels were detected by Western blotting using a mouse M2 anti-FLAG primary antibody (Sigma-Aldrich) and an anti-mouse IgG secondary antibody conjugated with horseradish peroxidase (HRP) (GE Healthcare). The analyzed channel constructs have a C-terminal FLAG tag epitope (DYKDDDDK). Chemiluminescent detection was performed using the Amersham ECL Western blotting detection kit (GE Healthcare). Exposure times were between 1 and 30 min. Images were then digitally acquired.

Recording apparatus

cGMP-gated currents from excised patches in inside-out configuration were recorded, with a patch-clamp amplifier (Axopatch 200B, Axon Instruments Inc., Foster City, CA, USA), 4–6 days after RNA injection, at room temperature (20–24°C). The perfusion system was as previously described (Sesti et al. 1995) and it allowed a complete solution change in less than 1 s. Borosilicate glass pipettes had resistances of 3–10 MΩ in symmetrical standard solution. The standard solution on both sides of the membrane consisted of (in mM) 110 NaCl, 10 HEPES and 0.2 EDTA (pH 7.4). The membrane potential was usually stepped from 0 to ±60 mV. We used Clampex 8.0, Clampfit 9.2, and Matlab 7.1 for data acquisition and analysis. Currents were low-pass filtered at 2 kHz and acquired digitally at 5 kHz. The current inhibition was calculated as $1 - I_{res}/I_{cG}$ (where I_{res} is the residual current after application of drugs and I_{cG} is the control current in the presence of 1 mM cGMP).

Application of sulfhydryl-specific reagents

The effect of Cd^{2+} was tested by perfusing the intracellular side of the membrane with a standard solution without EDTA (to avoid partial Cd^{2+} chelation), supplemented with 200 µM of $CdCl_2$ (Becchetti and Roncaglia 2000; Roncaglia and Becchetti 2001; Mazzolini et al. 2002; Nair et al. 2006; Mazzolini et al. 2008) for 5 min, in the open (i.e., in the presence of 1 mM cGMP) and close state (i.e., in the absence of 1 mM cGMP). When a partial inhibition was observed after 5–7 min of Cd^{2+}, we investigated the effect of longer exposures to Cd^{2+} ions up to 10 min.

Cd^{2+} inhibition of mutant channels where exogenous cysteines are introduced in specific locations can have a high efficacy with a half inhibition constant $K_{1/2}$ varying between 100 nM and 1 µM (Rothberg et al. 2003); in mutant channels H462C + Q468C constructed in the HCN channels Cd^{2+} inhibition has a value of $K_{1/2}$ of 72 nM (Rothberg et al. 2003). Similarly, Cd^{2+} inhibition of mutant channels T360C and I361C constructed in the CNGA1 channels occurs with a $K_{1/2}$ in the micromolar range and develops in just a few seconds (Contreras et al. 2008). The high efficacy of Cd^{2+} inhibition in these mutant channels is explained by its coordination to three and possibly four exogenous cysteines forming a stable and rigid binding site. In other conditions, Cd^{2+} inhibition has a lower efficacy and develops on a longer time scale (Yellen et al. 1994; Kurz et al. 1995; Krovetz et al. 1997; Liu et al. 1997; Kubo et al. 1998; Becchetti and Roncaglia 2000). The lower efficacy of Cd^{2+} inhibition in these mutant channels is caused by the Cd^{2+} coordination to the S atom of only two cysteines—either exogenous or endogenous—and the longer time scale is caused by concomitant fluctuations of coordinating cysteines (Krizek et al. 1993; Berg and Godwin 1997).

The time course of Cd^{2+} inhibition of mutants Q409C and A414C was determined with the application of 100 and 200 μM of the reagent in the closed state for variable periods and by measuring the current observed after Cd^{2+} removal and in the presence of 1 mM cGMP. Figure 1a shows data collected from seven patches containing mutant channel Q409C exposed for variable time periods to 100 (filled circles) and 200 µM Cd^{2+} (open circles), respectively. Data were normalized to the cGMP current activated at +60 mV, before Cd^{2+} treatment. The solid line through the experimental points was obtained from the equation $\exp(-\tau/t)$, where τ is the time constant of Cd^{2+} inhibition. Figure 1b shows similar data but for mutant channel A414C (six patches). The time constant of Cd^{2+} inhibition was 909 and 217 s for 100 and 200 µM Cd^{2+} for mutant channel Q409C and was 555 and 105 s for 100 and 200 µM Cd^{2+} for mutant channel A414C.

Therefore, we analyzed Cd^{2+} inhibition in the closed state by exposing patches to 200 µM Cd^{2+} for 5 min. Following this procedure, in some constructs such as Q409C + C505T and Q409C + C481A, an inhibition between 30 and 70% was observed. In order to check whether a partial inhibition that was observed after 5 min of Cd^{2+} exposure was due to a slow inhibition rate of Cd^{2+} ions, we investigated the effect of longer exposures to Cd^{2+} ions. To study Cd^{2+} inhibition in the open state, we applied 200 µM Cd^{2+} ions in the presence of 1 mM cGMP for 5 min or longer, during which the amplitude of the cGMP-activated current was continuously monitored. If after 5 min of Cd^{2+} exposure, the amplitude of the cGMP current did not change by more than 10%, we concluded that Cd^{2+} ions did not inhibit the cGMP-activated current.

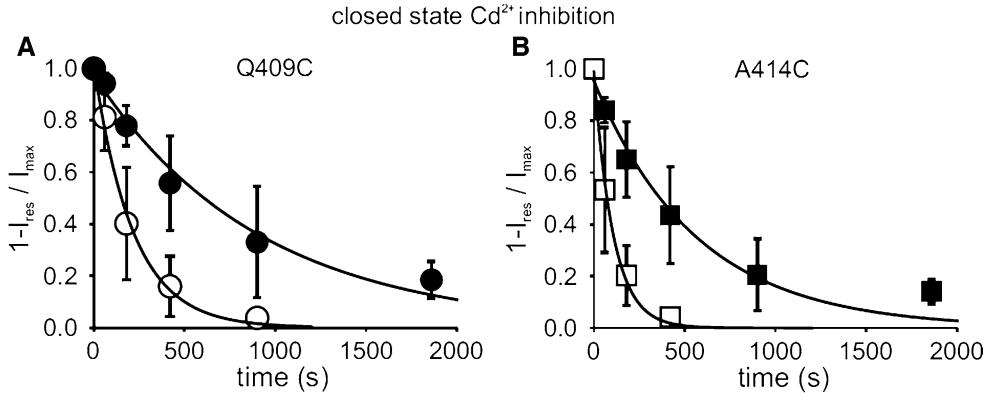

Fig. 1 Time course of Cd^{2+} closed-state inhibition and estimation of the distance between C_α of coordinating cysteines. **a**, **b** Time-dependent inhibition of mutant channels Q409C and A414C by 100 μM (*closed symbols*) and 200 μM (*open symbols*) Cd^{2+}, respectively, in the closed state. Data are shown as mean ± standard deviation (SD). *Solid line* through the experimental points was obtained by fitting the data with $\exp(-\tau/t)$, where τ is the time constant of Cd^{2+} inhibition

Cross-linker compounds (M-2-M and M-4-M) were dissolved in dimethyl sulfoxide (DMSO) and diluted in a standard solution reaching a final concentration of 100 μM. The final concentration of DMSO was 0.1%. We also checked that this concentration of DMSO did not affect the cGMP-activated current. Solutions containing cross-linker compounds were prepared immediately before application (typically <5 min) to prevent degradation, as these reagents dissociate rapidly in aqueous solution; in fact, they were never used for more than 45 min after dissolution. Cross-linkers of different length were used to determine the distance between exogenously introduced cysteines (Ren et al. 2006; Loo and Clarke 2001). In experiments with mutant channel Q409C, after application of 100 μM M-2-M in the open state, 5 mM, DTT was applied for at least 10 min in order to check whether the blocking effect caused by M-2-M was reversible.

Estimation of the distance between C_α of coordinating cysteines

MTS cross-linkers, such as M-2-M and M-4-M, and Cd^{2+} modify cysteine mutant channels by triggering different mechanisms and the comparison of their effect are used as a tool for the investigation of conformational changes during channel gating (Mazzolini et al. 2002, 2008; Craven et al. 2008). Indeed, the MTS cross-linkers bears reactive S atoms at both ends and forms covalent bonds with two cysteines from different subunits (Loo and Clarke 2001) whereas one Cd^{2+} ion usually coordinates two or even more cysteines (Benitah et al. 1996; Holmgren et al. 1998; Loussouarn et al. 2000).

In order to evaluate the distance between the C_α of cysteines coordinating Cd^{2+} ions or the cross-linkers, we performed an extensive in silico search. We explored possible 3-D conformations of Cd^{2+}, M-2-M and M-4-M interacting with two cysteines in which $-NH_2$ and –COOH functional groups had been substituted by $-CH_3$. This substitution was made in order to avoid polar interactions that could alter the probability of sampled conformational states. Initial structures were generated by means of PRODRG server (Schuettelkopf and van Aalten 2004). Bonded and van der Waals parameters of the force field were obtained from the generalized Amber force field (GAFF) (Wang et al. 2004). Atomic partial charges and Cd–S distances for the Cd^{2+} complex were calculated by optimizing the initial structure and using the DFT/B3LYP methodology (Becke 1993) followed by RESP fitting (Bayly et al. 1993). Molecular orbitals were described by the 6-31G(d) type basis set for H, C and S atoms (Binkley et al. 1980) and the LANL2DZ basis set with effective core potentials for Cd atom (Hay and Wadt 1985). Calculations were made using the Gaussian03 program (Gaussian, Inc., Wallingford, CT). Atomic partial charges for the M-2-M and M-4-M derivates were evaluated with Gasteiger charge calculations (Gasteiger and Marsili 1980).

After brief minimization, we performed molecular dynamics (MD) simulations using the AMBER8 program (Pearlman et al. 1995) for 100 ns with a time step of 1 fs and collecting snapshots every 10 ps. Temperature was maintained at 300 K by coupling the systems to a Berendsen thermostat (Berendsen et al. 1984). Solvation was considered by means of the generalized Born/surface area model (Still et al. 1990). Bonds containing hydrogens were kept fixed with the SHAKE algorithm (Ryckaert et al. 1977).

From the analysis of the conformations sampled by MD, it is possible to infer the possible distance between the C_α of cysteines (Fig. 2). Hence, if Cd^{2+} inhibits the channel by coordinating to two cysteines, the distance between the C_α of coordinating cysteines is $\leq$10.5 Å. If channel inhibition is observed with M-2-M but not with Cd^{2+} the distance

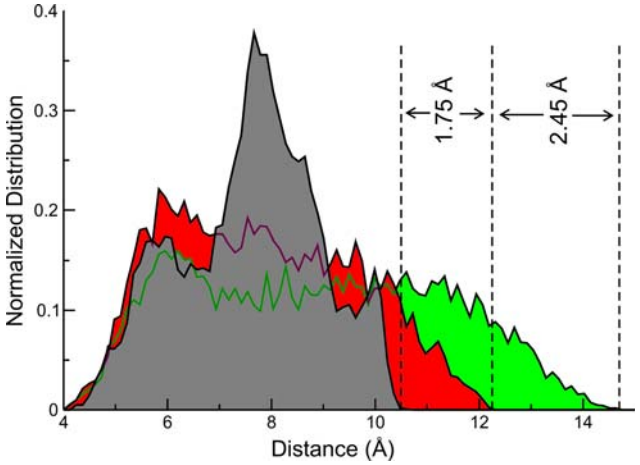

Fig. 2 Normalized distribution of the distance between the C_α of cysteines coordinating Cd^{2+} ions (*gray*), M-2-M (*red*) or M-4-M (*green*) as evaluated from MD simulations

between the C_α of coordinating cysteines is between 10.5 and 12.3 Å. Similarly, if the inhibition is caused by M-4-M and not by Cd^{2+} and M-2-M, the distance of the C_α of coordinating cysteines is between 12.3 and 14.7 Å.

Sequence and structural analysis of the CNB domains

The 3-D structure of the CNB domains from six different proteins is available in the Protein Data Bank (PDB) (Berman et al. 2000): the CNB domain of CAP (entry 1G6 N) (Passner et al. 2000), KAP0 (entries 1NE6 and 1RL3) (Wu et al. 2004a, b), KAP3 (entry 1CX4) (Diller et al. 2001), HCN2 (entries 1Q3E and 1Q5O) (Zagotta et al. 2003), *M. loti* CNB domain mutant (MlotiK1) (entries 1U12 and 1VP6) (Clayton et al. 2004) and CNGC6 (entry 1WGP) (Chikayama E, Nameki N, Kigawa T, Koshiba S, Inoue M, Tomizawa T, Kobayashi N, Yokoyama S, unpublished). All sequence alignments were performed with Clustal W (Thompson et al. 1994). Structural superimpositions were performed by using the program STAMP (Russell and Barton 1992).

Structural models of CNGA1 C-linker and CNB domains were built by using homology modeling with the program Modeller 6v1 (Šali and Blundell 1993). In some cases, additional restraints on the C_α–C_α distances of selected amino acids were used, according to the experimental observations in the present manuscript.

Results

A common tool for the investigation of functional and structural properties of ionic channels is Scanning Cysteine Mutagenesis (SCM) in which residues in a given region of the ionic channel are mutated one by one into cysteines and the action of reagents able to interact with the sulfur atom of the single cysteine is investigated. Considering this rationale, we scanned several residues in the C-linker domain of CNGA1 channels from F375 to H420. In these mutated channels, we studied the effect that 200 μM Cd^{2+} added to the bathing medium in the presence (open state) or in the absence (closed state) of 1 mM cGMP had on cGMP-activated current. Exposure of CNGA1 channel to 200 μM Cd^{2+} induced a very small permanent change in the cGMP-activated current ($9.4 \pm 6.0\%$, $N = 7$) (Nair et al. 2006). During this extensive SCM, we found that many mutant channels (F380C, V391C, N400C, N402C, A403C, A404C, A406C, E407C, F408C, Q409C, A414C and Q417C) were irreversibly inhibited by Cd^{2+} ions (the nomenclature adopted here for the mutants in the CNGA1, $CNGA1_{cys\text{-}free}$ and tandem backgrounds is described in the "Materials and methods" section).

In the present manuscript, we analyze in detail the molecular mechanisms underlying Cd^{2+} inhibition and longer cross-linkers such as M-2-M and M-4-M in mutant channels Q409C and A414C using the rationale previously described.

Cd^{2+} inhibition of mutant channel A414C

The CNGA1 channel is composed of four subunits, each showing six-transmembrane-helix topology. Each subunit contains seven native or endogenous cysteines: C35, C169, C186, C314, C481, C505 and C573. C35 is located near the N-terminal of the CNGA1 channel, at the cytoplasmic side (Molday et al. 1991; Brown et al. 1998), and it is thought to interact with C481 in the open state, but not in the closed state (Gordon et al. 1997; Rosenbaum and Gordon 2002). C169 and C186 are located in the S1 and their functional and/or structural role has not been studied in detail, yet. C314 in the S5 transmembrane segment can interact with residues at position 380 in the S6 domain (Nair et al. 2006). C481 is located in the C-linker region (Brown et al. 1998) and its role in channel function has been extensively studied (Brown et al. 1998). C505 in the CNB domain is accessible to sulfhydryl reagents in the closed state but not in the open state (Sun et al. 1996; Matulef et al. 1999). Finally, C573 is located near the C-terminus of the channel. C573 does not contribute to the potentiation observed after the application of compounds promoting the formation of disulfide bonds (Gordon et al. 1997) and does not seem to have any structural and functional role. Therefore, we studied the effects of mutations in the C-linker region and in the CNB domain limiting our analysis only to C481 and C505.

When the CNGA1 channel of bovine rod is exposed for some minutes to an intracellular medium containing 200 μM Cd^{2+} in the open or closed state, the cGMP-activated current measured after Cd^{2+} removal is not significantly modified, as shown in Fig. 3a (Becchetti and

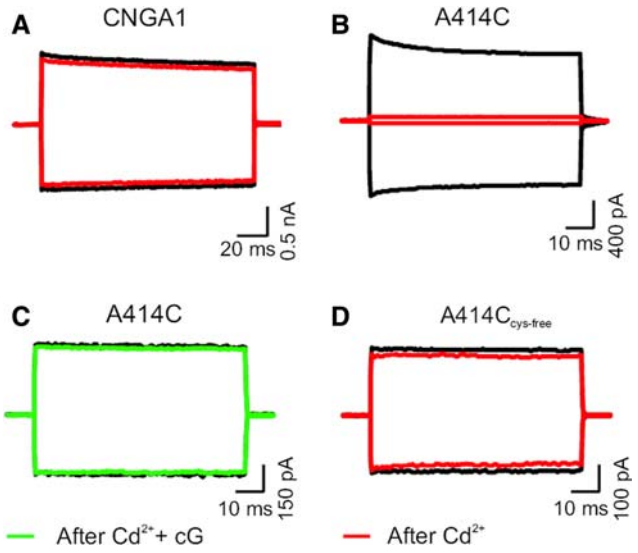

Fig. 3 Effect of Cd^{2+} on the CNGA1 and mutant channels. **a** Effect of 200 μM Cd^{2+} on the CNGA1 channel in the closed state. **b**, **c** Effects of 200 μM Cd^{2+} on mutant channel A414C in the closed and open state, respectively. Cd^{2+} inhibits irreversibly mutant channel A414C (**b** *red trace*) in the closed state but not in the open state (**c** *green trace*). **d** Effect of 200 μM Cd^{2+} on the mutant $Q409C_{cys\text{-}free}$ (mutation in the cysteine free background) in the closed state. Currents were measured in the presence of 1 mM cGMP before and after a 5-min exposure to 200 μM Cd^{2+}. Current traces were obtained by stepping the membrane voltage from 0 to ±60 mV. *Black traces* were obtained in control conditions, before the application of Cd^{2+}, and *red traces* after the application of Cd^{2+} in the closed state—absence of cGMP. *Green traces* were obtained after the application of Cd^{2+} in the open state and in the presence of 1 mM cGMP

Roncaglia 2000; Nair et al. 2006). The absence of any irreversible effect indicates that in the CNGA1 either Cd^{2+} ions cannot coordinate with multiple cysteines and histidines or such coordination does not modify the channel gating. A different behavior was observed when a cysteine was introduced at position 414. In fact, as shown in Fig. 3b, the mutant channel A414C was irreversibly inhibited by exposure to Cd^{2+} ions in the closed state. The irreversible inhibition of the mutant channel A414C by 200 μM Cd^{2+} was 96.4 ± 2.7% ($N = 7$). As shown in Fig. 3c, mutant channel A414C was not inhibited by Cd^{2+} in the open state (2.6 ± 2.0%, $N = 4$), where neither the cross-linker M-2-M nor M-4-M inhibited the mutant channel A414C in the open state (data not shown). These results suggest that in the open state 414C of different subunits are far from each other and they are also distant from endogenous C481 and C505. Irreversible inhibition (10.1 ± 2.1%, $N = 2$) in the closed state was not observed when A414 was substituted by a cysteine in the $CNGA1_{cys\text{-}free}$ channel (Matulef et al. 1999), as shown in Fig. 3d.

The different blocking effect of Cd^{2+} ions in the closed state observed in mutant channels A414C and $A414C_{cys\text{-}free}$ can be produced either by two different mechanisms or by their combination. Cd^{2+} inhibition of cysteine mutants in the CNGA1 background can originate from Cd^{2+} coordination with endogenous cysteines and particularly with C481 and C505 which are known to be part of the C-linker and the CNB domains, respectively, and are involved in the gating machinery of CNGA1 channels (Brown et al. 1998). An alternative explanation is that the 3-D structure of $CNGA1_{cys\text{-}free}$ channels differs by a few Å from that of CNGA1 channels (Mazzolini et al. 2008), so that Cd^{2+} can coordinate exogenous cysteines introduced in the CNGA1 channels but not in the $CNGA1_{cys\text{-}free}$ channels. Zagotta and co-workers have shown that tetracaine blocks in a very similar way both the CNGA1 and $CNGA1_{cys\text{-}free}$ channels, although also that the concentration of CNG activating half of the maximal current is different in the two channels (Matulef et al. 1999). Therefore, some physiological properties of the $CNGA1_{cys\text{-}free}$ are very similar to those of the CNGA1 channels, but the degree of similarity of the 3-D structure of the CNGA1 and $CNGA1_{cys\text{-}free}$ has not been established. Experiments from our lab show that removal of all cysteines from the CNGA1 channels perturbs the position of several residues and that, for some amino acids, the relative distance between homologous residues in different subunits varies by some Å in the two channels (Mazzolini et al. 2008). Given the major structural role of cysteines in protein structure, it is expected that the exact 3-D structure of a native protein is going to be different—to some extent—from its cysteine-free version.

Therefore, we decided to analyze Cd^{2+} inhibition in mutant channels Q409C and A414C in the CNGA1 channel background. Given their probable proximity to Q409 and A414, we concentrated our attention to the two endogenous C481 and C505 and we investigated the mechanism of the irreversible Cd^{2+} inhibition observed in the closed state of mutant channel A414C by comparing Cd^{2+} inhibition whilst C481 was replaced with an alanine and C505 was replaced with a threonine. The inhibition caused by the exposure to 200 μM Cd^{2+} in A414C was not significantly affected in the double mutant A414C + C481A (Fig. 4a), but it was drastically reduced in the double mutant A414C + C505T (Fig. 4b). Moreover, we tried to analyze the effect of Cd^{2+} in triple mutant channels A414C + C481A + C505T, but, unfortunately, we were not able to record any cGMP-activated current from these mutants even in the presence of 5 mM DTT. In order to test the possibility that Cd^{2+} inhibition of mutant A414C is mediated by its coordination to native C505 and exogenous cysteine at position 414, we inserted a cysteine at position 505 in the mutant $A414C_{cys\text{-}free}$. As shown in Fig. 4c, 200 μM Cd^{2+} ions irreversibly inhibited also in mutant channel A414C + $C505_{cys\text{-}free}$.

As shown in Fig. 4d, 200 μM Cd^{2+} ions inhibited the mutant channel A414C by 96.4 ± 2.7% ($N = 7$), the double

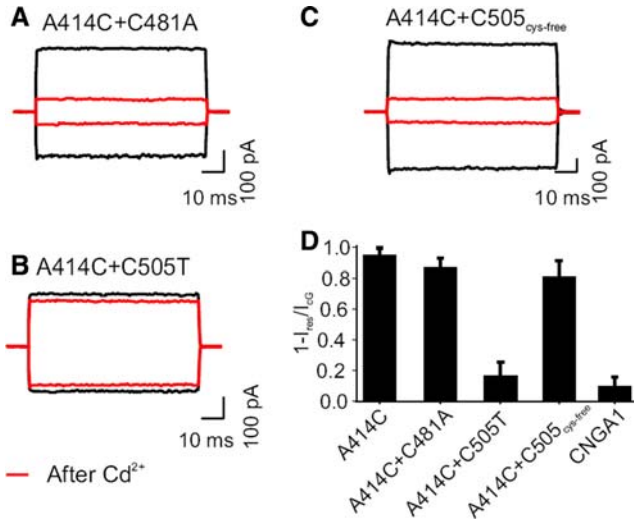

Fig. 4 Closed-state inhibition of mutant channel A414C depends on C505. **a–c** Current recordings of cGMP-activated current before (*black*) and after (*red*) application of 200 μM Cd^{2+} in the closed state from mutant channels A414C + C481A, A414C + C505T and A414C + $C505_{cys\text{-}free}$, respectively. Voltage commands as in Fig. 3. **d** *Bar plot* of the average inhibition by 200 μM Cd^{2+} of mutant channels in the closed state. Data shown as mean ± SD

mutant channel A414C + C481A by 86.0 ± 6.2% ($N = 5$) and the mutant A414C + $C505_{cys\text{-}free}$ by 81 ± 10% ($N = 4$). In contrast, Cd^{2+} inhibition was drastically reduced and almost eliminated in the double mutant A414C + C505T (18.0 ± 7.2%, $N = 3$) which was not statistically different from that observed in the CNGA1 channel (9.4 ± 6.0%, $N = 12$). These results strongly indicate that Cd^{2+} inhibition in the closed state in A414C mutant channels was generated by its coordination with 414C and C505 (for clarity, native residues will be indicated throughout the text by swapping the 1-letter codes and position numbers, i.e., 414C, with respect to the common notation, here adopted for native residues, i.e. C505).

The interaction between C505 and exogenous cysteine A414C is within the same subunit

In order to establish whether Cd^{2+} inhibition observed in the closed state in mutant A414C was a consequence of a cross-linkage between two cysteines from the same subunit or from neighboring subunits, two tandems were constructed: the tandem A414C + C505T/CNGA1 where each subunit contained either an exogenous cysteine at 414 or the native cysteine 505, and the tandem A414C/C505T where two subunits have 414C as well as C505 and the other two have A414 and 505T. As shown in Fig. 5a, 200 μM Cd^{2+} in the absence of cGMP poorly inhibited the tandem construct A414C + C505T/CNGA1 and Cd^{2+} inhibition was very similar to what observed in the CNGA1 channel.

As summarized in Fig. 5b, while 200 μM Cd^{2+} ions almost completely inhibited the cGMP-activated current in mutant channel A414C, it did not significantly inhibit the tandem A414C + C505T/CNGA1 (5.6 ± 2.0%, $N = 4$) even during exposures lasting up to 20 or 30 min. In contrast, Cd^{2+} application inhibited the A414C/C505T channel similarly to what observed in the A414C channel. From these results, we conclude that the inhibition in mutant channel A414C in the closed state in the presence of Cd^{2+} is caused by its cross-linkage between C505 and 414C of the same subunit.

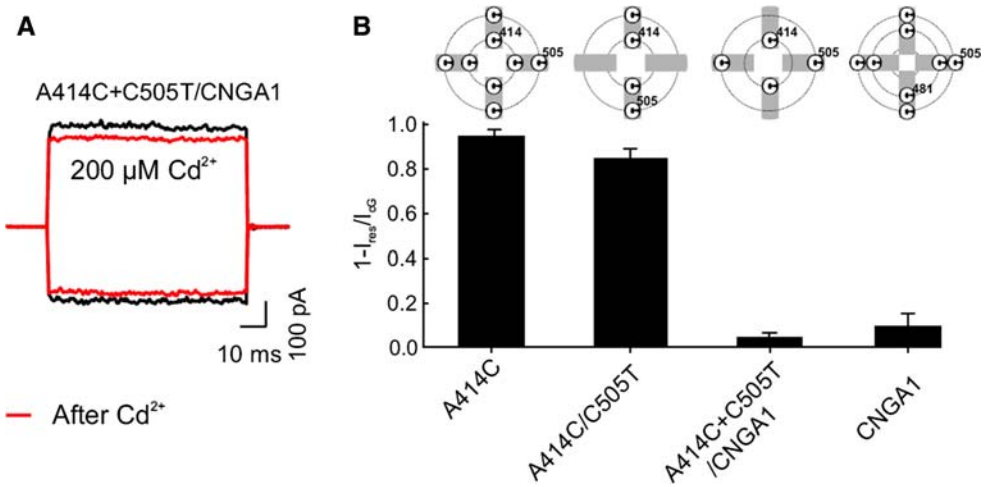

Fig. 5 The interaction between C505 and 414C is within the same subunit. **a** Current recordings before (*black*) and after (*red*) application of 200 μM Cd^{2+} in the closed state from mutant channel A414C + C505T/CNGA1. Voltage commands as in Fig. 2. **b** *Bar plot* of the average inhibition by 200 μM Cd^{2+} in the closed state. Application of 200 μM Cd^{2+} at the intracellular side of the membrane patch inhibited the cGMP-activated current by 84.0 ± 6.1% in A414C/C505T and by 5.6 ± 2.0% in A414C + C505T/CNGA1. The representation at the *top of each bar* shows the cysteines present in each subunit

Open state inhibition of mutant channel Q409C

During the SCM analysis in the C-linker region we found that a majority of mutant channels in the open state were not inhibited by thiol-specific reagents. Neither Cd^{2+} nor long cross-linkers such as those of the M-X-M family produced any significant permanent inhibition of the cGMP-activated current. A remarkable exception was mutant channel Q409C, which was permanently inhibited by 100 μM M-2-M. Exposure to 200 μM Cd^{2+} ions in the open state poorly inhibited (16.0 ± 2.1%, $N = 4$) the cGMP-activated current (see Fig. 6a).

In contrast, as shown in Fig. 6b, when, in the open state, 100 μM M-2-M was added, the cGMP-activated current recorded from the mutant channel Q409C was permanently inhibited. Inhibition persisted even after the patch was washed for 10 min or longer with a medium not containing thiol reagents. To check whether blockage of the cGMP-gated current in the mutant channel Q409C was caused by the formation of disulfide bonds between S atoms of M-2-M and of exogenous cysteines in position 409, after treatment with M-2-M we exposed the patch to 5 mM DTT. After 10 min of exposure to this reducing agent the cGMP-gated current recovered to 70 ± 12% ($N = 4$) of the initially observed current (Fig. 6b). During the exposure to M-2-M, the cGMP-activated current declined within 4–6 min with an average time constant of about 255 s, as shown in Fig. 6c. In order to identify the molecular mechanisms underlying this open state inhibition, we analyzed the effect of 100 μM M-2-M on mutant channel Q409C when C505 was replaced with a threonine. As shown in Fig. 6d, the compound M-2-M did not inhibit the double mutant channel Q409C + C505T (10 ± 7%, $N = 4$). Therefore, inhibition of Q409C in the open state caused by the compound M-2-M is due to its cross-linking to 409C and C505. In order to establish whether the inhibition was a consequence of the cross-linkage between two cysteines from the same subunit or from neighboring subunits, M-2-M inhibition in the open state was analyzed in the tandem Q409C + C505T/CNGA1. In this tandem construct, each subunit contained either 409C or C505 and the cross-linkage between 409C and the C505 can occur only between different subunits. As shown in Fig. 6e, M-2-M in the open state did not inhibit the tandem construct Q409C + C505T/CNGA1.

As summarized in Fig. 6f, 100 μM M-2-M in the open state inhibited 86 ± 6% ($N = 5$) of the cGMP-activated current in mutant channel Q409C, but only 10 ± 7% ($N = 4$) in the double mutant Q409C + C505T and 17 ± 10% ($N = 4$) in the tandem construct Q409C + C505T/CNGA1. It is concluded that inhibition of mutant channel Q409C by the compound M-2-M in the open state is caused by the cross-linkage of C505 with 409C of the same subunit.

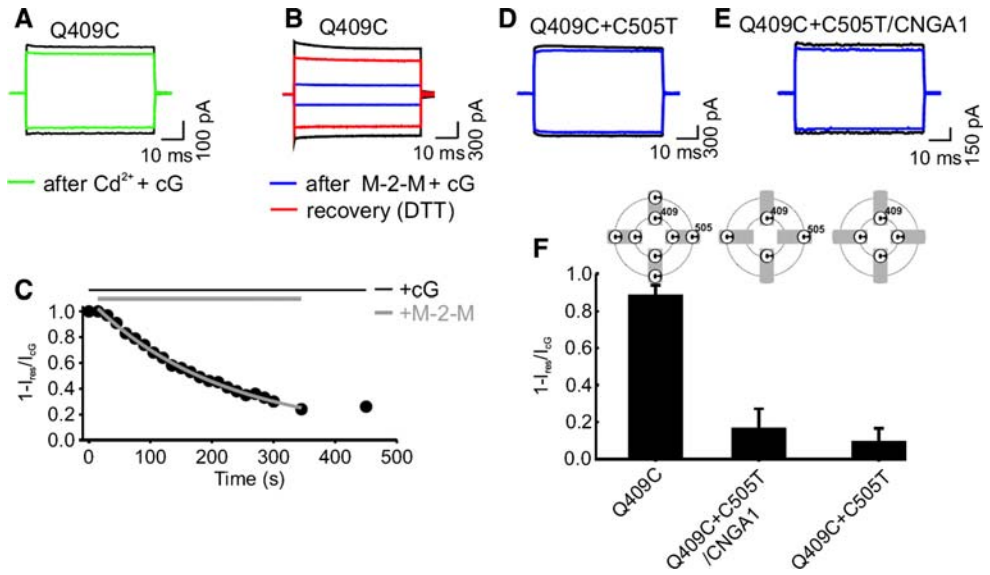

Fig. 6 Q409C is inhibited by M-2-M in the open state. **a** Current recordings obtained in the presence of 1 mM cGMP before (*black*) and after (*green*) exposure to 200 μM Cd^{2+} in the open state. **b** Current recordings obtained in the presence of 1 mM cGMP before (*black*) and after (*blue*) exposure to M-2-M in the open state; recovery after exposure of 5 mM DTT (*red*). **c** Time course of inhibition of mutant channel Q409C by M-2-M in the open state. The *gray line* through the experimental points was obtained by fitting with $\exp(-\tau/t)$, where τ is the time constant of M-2-M inhibition. **d**, **e** Effect of M-2-M in the open state on Q409C + C505T and Q409C + C505T/CNGA1 channels, respectively. Colors of current recordings correspond to the same parameters as in **b**. Voltage commands as in Fig. 3. **f** *Bar plot* of average inhibition by 100 μM M-2-M in the open state. A 5-min application at the intracellular side of the membrane patch inhibited the cGMP-activated current by 87 ± 6% in Q409C, by 17 ± 10% in Q409C + C505T/CNGA1 and by 10 ± 7% in Q409C + C505T. The representation at the *top of each bar* shows the cysteines present in each subunit

Cd^{2+} inhibition of mutant channel Q409C in the closed state

Mutant channel Q409C was permanently inhibited by the exposure to 200 μM Cd^{2+} also in the closed state, as shown in Fig. 7a. The irreversible inhibition observed in the closed state was not seen when Q409 was substituted with a cysteine in the $CNGA1_{cys\text{-}free}$ (see Fig. 7b).

In order to understand the molecular mechanisms underlying Cd^{2+} inhibition in the closed state in mutant channel Q409C, we analyzed the inhibition when C481 was replaced with an alanine and C505 was replaced with a threonine. Exposure to 200 μM Cd^{2+} for 5 min inhibited the cGMP-activated current in the double mutant channels Q409C + C481A and Q409C + C505T between 30 and 50%. When membrane patches were exposed to 200 μM Cd^{2+} for at least 15 min an almost complete blockage of the cGMP-activated current was detected, as shown in Fig. 7c and d. Moreover, we tried to analyze the effect of Cd^{2+} in triple mutant channels Q409C + C481A + C505T, but we were not able to record any cGMP-activated current from these mutant channels even in the presence of 5 mM DTT.

We engineered the tandem construct Q409C + C505T/CNGA1, having a cysteine residue at position 409 in all four subunits, but native C505 present in only two subunits. In this tandem construct, Cd^{2+} inhibition was drastically reduced and was comparable to that observed in the CNGA1 channels. In this construct, the four native C481 were present, and the negligible Cd^{2+} inhibition indicated a minor role of the native C481. In contrast, Cd^{2+} inhibition in the tandem Q409C + C505T/Q409C was very similar to that observed in mutant channel Q409C.

Figure 7e compares the inhibition caused by 200 μM Cd^{2+} in the closed state in different constructs: the largest inhibition (98.5 ± 1.9%, $N = 5$) was observed in mutant channel Q409C, where the exogenous cysteine at position 409 is present in all four subunits. A very similar inhibition (97.1 ± 2.4%, $N = 4$) was observed in the tandem construct Q409C + C505T/Q409C where the native C505 was replaced with a threonine in two subunits. In the double mutants Q409C + C481A and Q409C + C505T, Cd^{2+} inhibition following an exposure of 5 min was reduced to 59.6 ± 6.4% ($N = 4$) and to 41.0 ± 3.2% ($N = 4$), respectively, but it was almost complete for exposures longer than 15 min. Cd^{2+} inhibition was very small (2.3 ± 2.1%, $N = 4$) in the tandem construct Q409C + C505T/CNGA1 where only two subunits have an exogenous cysteine at position 409. A similar negligible Cd^{2+} inhibition (9.4 ± 6.0%, $N = 7$) was observed in the CNGA1 channel. Cd^{2+} inhibition is significantly slower in the double mutants Q409C + C481A and Q409C + C505 and it was abolished in the tandem construct Q409C + C505T/CNGA1.

In order to obtain further information on the mechanisms leading to Cd^{2+} inhibition of mutant Q409C in the closed state, we inserted a cysteine at position 505 in the mutant $Q409C_{cys\text{-}free}$. However, we were not able to record any cGMP-activated current from this mutant channel even in the presence of 5 mM of the reducing compound DTT. To determine the cause of the absence of cGMP-gated current, we performed a biochemical analysis using oocytes injected with the mRNA of the above mentioned mutant channel. The total protein from injected oocytes was solubilized and ran on SDS-PAGE gels under either non-reducing or reducing (Fig. 7f) conditions, and channel proteins were

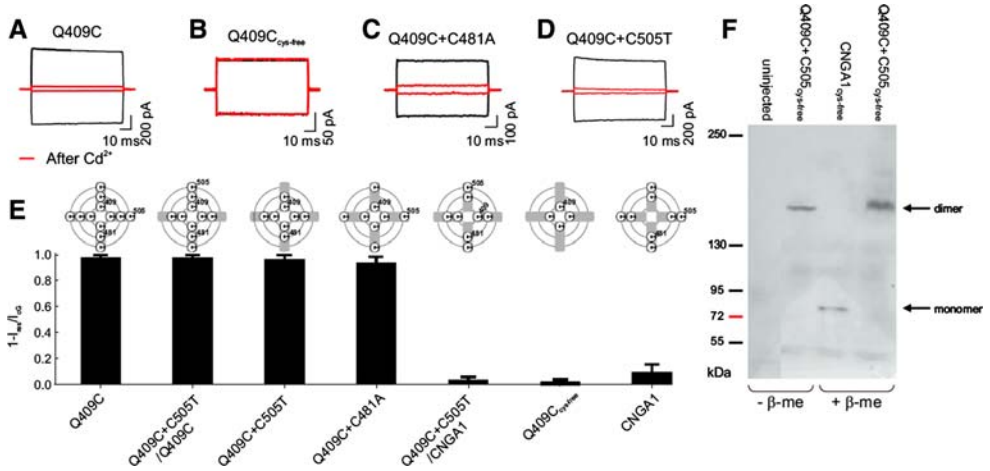

Fig. 7 Closed-state inhibition of Q409C by Cd^{2+} depends on C505 and C481. **a–d** Current recordings of cGMP-activated current before (*black*) and after (*red*) closed state application of 200 μM Cd^{2+} on mutant channels Q409C, $Q409C_{cys\text{-}free}$, Q409C + C481A and Q409C + C505T respectively. Voltage commands as in Fig. 3. **e** *Bar diagram* comparing the inhibition of 200 μM Cd^{2+} in constructs containing cysteines in different locations. Data shown as mean ± SD. The representation at the *top of each bar* shows the cysteines present in each subunit. **f** Biochemical analysis of mutant channel $Q409C + C505_{cys\text{-}free}$. Western blot of total proteins from *Xenopus* oocytes, either uninjected, injected with the mRNA of $CNGA1_{cys\text{-}free}$ channels (control) and $Q409C + C505_{cys\text{-}free}$ mutant channels

visualized using Western blotting. As shown in Fig. 7f, the $CNGA1_{cys\text{-}free}$ channel ran at the size of a monomer (80 kDa). In contrast, the mutant channel Q409C + $C505_{cys\ free}$ ran at the size of a dimer (160 kDa) both under reducing and non-reducing conditions. Therefore, we concluded that the absence of cGMP-dependent current in mutant channels Q409C + $C505_{cys\text{-}free}$ was likely to be caused by the formation of disulfide bonds that interfered/impeded with the normal trafficking to the cell membrane or with the correct function of the protein.

These results show that Cd^{2+} inhibition in mutant channel Q409C cannot be ascribed to Cd^{2+} coordination between the exogenous cysteine and one native cysteine in the same subunit as happens for mutant channel A414C. Therefore, it is possible that inhibition in mutant channel Q409C is mediated also by Cd^{2+} coordination to cysteines belonging to different subunits.

Discussion

In the present article, we have investigated the relative distance between specific residues in the C-linker of CNGA1 channels. These interactions were analyzed by introducing cysteines into selected positions and by studying the effect of thiol specific reagents such as Cd^{2+} and different MTS cross-linkers (Loo and Clarke 2001). We found that mutant channels Q409C and A414C are irreversibly inhibited in the closed state by 200 µM Cd^{2+} added at the intracellular side of the membrane. In contrast, in the presence of 1 mM cGMP, these two channels are not inhibited by Cd^{2+} ions, but the mutant channel Q409C is powerfully inhibited by the cross-linker reagent M-2-M. Cd^{2+} inhibition of mutant channels Q409C and A414C has a lower efficacy with respect to other channels and develops with a time constant of the order of hundreds of seconds (Yellen et al. 1994; Kurz et al. 1995; Krovetz et al. 1997; Liu et al. 1997; Kubo et al. 1998; Becchetti and Roncaglia 2000).

Our results shows that residues C505 and A414 of the same subunit are located at a distance between 4 and 10.5 Å (Fig. 2) in the closed state whereas in the open state C505 moves towards the residue Q409 of the same subunit. The molecular mechanisms underlying these effects imply that the molecular architecture of the C-linker and CNB domain in CNGA1 channels is not consistent with the 3-D structure of HCN2 channels neither in the open nor in the closed state as it will be discussed hereafter.

Cd^{2+} and M-2-M inhibition in mutant channels Q409C and A414C

In the closed state 200 µM Cd^{2+} powerfully inhibited mutant channels Q409C and A414C (Fig. 1a, b). Inhibition of mutant channel A414C was not affected by the replacement of C481 with an alanine, but was abolished when C505 was replaced with a threonine (Fig. 4) and in mutant channel $A414C_{cys\text{-}free}$ (Fig. 3d). Cd^{2+} inhibition (Fig. 4c) was present also in mutant channel A414C + $C505_{cys\text{-}free}$ confirming that Cd^{2+} inhibition is caused by its coordination to exogenous 414C and to C505. Cd^{2+} inhibition was also abolished in the tandem construct A414C + C505T/CNGA1 where each subunit had only one of the two cysteines

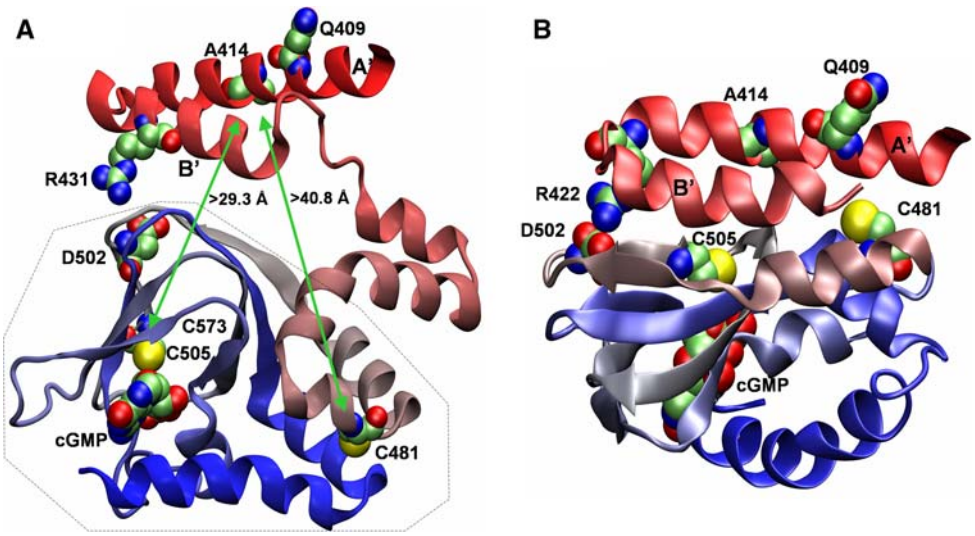

Fig. 8 Possible structures of the C-linker**. a** Homology model of the CNGA1 subunit using HCN2 (PDB entry 1Q3E) as a template. Helices are labelled alphabetically, strands are labelled numerically. The model shows that C505 and C481 are very far from either Q409 or A414. In contrast, R431 and D502 are close to each other and form a salt bridge, which is present also in the template and is very well conserved in the CNGA1-4 family. Structural models were built using the Modeller 6.2 program (Šali and Blundell 1993). **b** Homology model restrained according to the experimental observations, where A414 and Q409 are near C481 and C505 as shown in the present manuscript

at position 414 and 505 (Fig. 5a). Therefore, Cd^{2+} inhibition of mutant channel A414C is caused by its coordination with C505 and with 414C of the same subunit.

In contrast, Cd^{2+} inhibition in the closed state in mutant channel Q409C cannot be ascribed to a simple mechanism as in the case of mutant channel A414C. As shown in Fig. 7, Cd^{2+} inhibition was present in double mutant channels Q409C + C481A and Q409C + C505T (Fig. 7). The comparison of Cd^{2+} inhibition in different constructs, shown in Fig. 7, suggests that inhibition is mediated by its coordination with cysteines in different subunits. Therefore, Cd^{2+} inhibition in mutant channel Q409C in the closed state is mediated by Cd^{2+} coordination to several cysteines such as the exogenous 409C and native C481, with C505 in the same and different subunits.

In the open state, Cd^{2+} inhibition was not observed either in Q409C or in A414C mutant channels. In the open state, the cross-linker reagent M-2-M (Loo and Clarke 2001) powerfully inhibited the mutant channel Q409C (Fig. 6), but not the mutant channel A414C. M-2-M inhibition was abolished in the double mutant channel Q409C + C505T and in the tandem construct Q409C + C505T/CNGA1. These results indicate that M-2-M inhibition in the open state is mediated by the cross-linkage between 409C and C505 of the same subunit.

These results reveal that in the closed state the residue at position 414 is at a distance between 4 and 10.5 Å from C505 of the same subunit, so that one Cd^{2+} ion can coordinate C505 and 414C of the same subunit. In the open state, C505 moves to reach a distance that ranges between 10.5 and 12.3 Å towards residue Q409 of the same subunit so that M-2-M—but not Cd^{2+}—can cross-link them; C505 has been previously proven to be accessible to MTSEA in the closed state but not in the open state (Brown et al. 1998; Sun et al. 1996; Matulef et al. 1999); C481 moves towards A461 during channel opening (Islas and Zagotta 2006). All these results indicate a complex molecular rearrangement occurring in the CNB domain and in the C-linker during gating.

Possible 3-D structure of the C-linker and cyclic nucleotide binding domain

HCN2 and CNGA1 channels share a sequence identity of 35% in the CNB domain and C-linker region and could be expected to have the same 3-D architecture. Indeed, R590 and E617 forming a salt bridge in HCN2 channels (Zagotta et al. 2003) and the homologous R431 and D502 in CNGA1 channels interact almost identically. In addition, amino acids like K472, E502 and D542 (Craven and Zagotta 2004) which were indicated to be important for the HCN2 function, are very well conserved in the CNGA1-4 family. Nonetheless, a homology model of the C-linker and CNB domain of the CNGA1 channel based on the HCN2 template (see Fig. 8a) fails to explain the experimental results here described: in fact, in this homology model, the distance between the C_α of C481 and Q409 is more than 40 Å and the distance between the C_α of C505 and A414 is more than 29 Å: these distances are not in agreement with the estimates obtained in the present investigation.

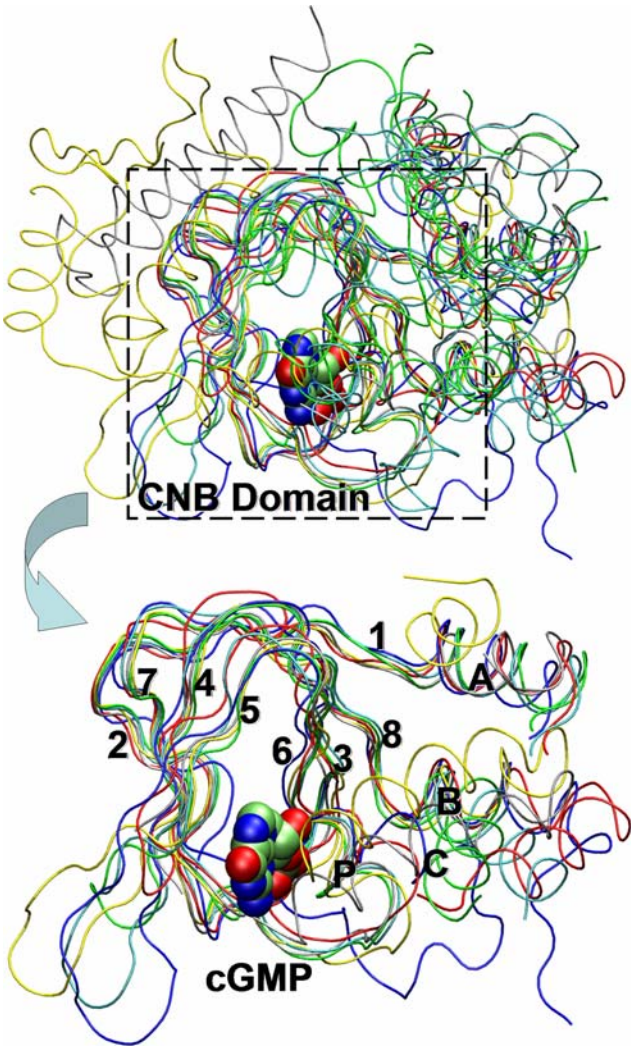

Fig. 9 Structural alignment of CNB domains of the proteins available in the PDB. Proteins are represented as tubes: *yellow* CAP (1GX6), *green* KAP0 (1NE6), *cyan* KAP3 (1CX4), *gray* HCN2 (1Q3E), *red* MlotiK1 (1VP6), *blue* CNGC6 (1WGP). CNB domain secondary structural elements are labelled alphabetically (helices) or numerically (strands). A cyclic nucleotide (cGMP, *sphere* representation) is also represented inside the binding site. Figure shows as the CNB domains are well structurally conserved, whereas the remainders of the proteins show higher structural variability

The 3-D structure of the CNB domains from six different proteins is available in the PDB (see "Materials and methods" section). These proteins share a sequence identity ranging between 13 and 45% and the overall protein architecture is very different; nevertheless the folding of their CNB domains is almost identical (Fig. 9). These considerations

indicate that the folding of the individual CNB domain is likely to be conserved among all or most of CNB proteins but the assembly of different subunits may be different. Therefore, differences between the 3-D structure of HCN2 and CNGA1 channels are likely to be residing in the structure of the C-linker domain and/or in the orientation of the single CNB domain subunits. Indeed, as shown in Fig. 8b, a rotation of the CNB domain around D502, towards the C-linker, can displace C481 and C505 near Q409 and A414 in order to satisfy the obtained experimental constraints. However, given the current uncertainties, it is not possible to infer the 3-D structure of the subunit with a high reliability. The exact molecular rearrangements underlying the transition from the closed to the open state will be determined by the combination of future structural and electrophysiological experiments.

Acknowledgments We thank Vincent Torre for the continuous support and very useful comments and suggestions and Anita Zimmerman for comments on the manuscript. We would like to thank Dr. Jessica Franzot for technical assistance and discussion in performing Western blot analysis. This work was supported by a HFSP grant, a COFIN grant (2006) from the Italian Ministry, a grant from CIPE (GRAND FVG) and a FIRB grant (RBLA03AF28_007) from MIUR.

References

Anselmi C, Carloni P, Torre V (2007) Origin of functional diversity among tetrameric voltage-gated channels. Proteins 66:136–146. doi:10.1002/prot.21187

Bayly CI, Cieplak P, Cornell WD, Kollman PA (1993) A well-behaved electrostatic potential based method using charge restraints for deriving atomic charges: the RESP model. J Phys Chem 97:10269–10280. doi:10.1021/j100142a004

Becchetti A, Roncaglia P (2000) Cyclic nucleotide-gated channels: intra- and extracellular accessibility to Cd2+ of substituted cysteine residues within the P-loop. Pflugers Arch 440:556–565

Becchetti A, Gamel K, Torre V (1999) Cyclic nucleotide-gated channels. Pore topology studied through the accessibility of reporter cysteines. J Gen Physiol 114:377–392. doi:10.1085/jgp.114.3.377

Becke AD (1993) Density-functional thermochemistry. III. The role of exact exchange. J Chem Phys 98:5648–5652. doi:10.1063/1.464913

Benitah JP, Tomaselli GF, Marban E (1996) Adjacent pore-lining residues within sodium channels identified by paired cysteine mutagenesis. Proc Natl Acad Sci USA 93:7392–7396. doi:10.1073/pnas.93.14.7392

Berendsen HJC, Postma JPM, van Gunsteren WF, Di Nola A, Haak JR (1984) Molecular dynamics with coupling to an external bath. J Chem Phys 81:3684–3690. doi:10.1063/1.448118

Berg JM, Godwin HA (1997) Lessons from zinc-binding peptides. Annu Rev Biophys Biomol Struct 26:357–371. doi:10.1146/annurev.biophys.26.1.357

Berman HM, Westbrook J, Feng Z, Gilliland G, Bhat TN, Weissig H, Shindyalov IN, Bourne PE (2000) The protein data bank. Nucleic Acids Res 28:235–242. doi:10.1093/nar/28.1.235

Biel M, Zong X, Ludwig A, Sautter A, Hofmann F (1999) Structure and function of cyclic nucleotide-gated channels. Rev Physiol Biochem Pharmacol 135:151–171. doi:10.1007/BFb0033672

Binkley JS, Pople JA, Hehre WJ (1980) Self-consistent molecular orbital methods. 21. Small split-valence basis sets for first-row elements. J Am Chem Soc 102:939–947. doi:10.1021/ja00523a008

Bradley J, Frings S, Yau KW, Reed R (2001) Nomenclature for ion channel subunits. Science 294:2095–2096. doi:10.1126/science.294.5549.2095

Brown RL, Snow SD, Haley TL (1998) Movement of gating machinery during the activation of rod cyclic nucleotide-gated channels. Biophys J 75:825–833

Chen TY, Illing M, Molday LL, Hsu YT, Yau KW, Molday RS (1994) Subunit 2 (or beta) of retinal rod cGMP-gated cation channel is a component of the 240-kDa channel-associated protein and mediates Ca^{2+}-calmodulin modulation. Proc Natl Acad Sci USA 91:11757–11761. doi:10.1073/pnas.91.24.11757

Chikayama E, Nameki N, Kigawa T, Koshiba S, Inoue M, Tomizawa T, Kobayashi N, Yokoyama S (2004) Solution structure of the cNMP-binding domain from Arabidopsis thaliana cyclic nucleotide-regulated ion channel (to be published)

Clayton GM, Silverman WR, Heginbotham L, Morais-Cabral JH (2004) Structural basis of ligand activation in a cyclic nucleotide regulated potassium channel. Cell 119:615–627. doi:10.1016/j.cell.2004.10.030

Contreras JE, Srikumar D, Holmgren M (2008) Gating at the selectivity filter in cyclic nucleotide-gated channels. Proc Natl Acad Sci USA 105(9):3310–3314

Craven KB, Zagotta WN (2004) Salt bridges and gating in the COOH-terminal region of HCN2 and CNGA1 channels. J Gen Physiol 124:663–677. doi:10.1085/jgp.200409178

Craven KB, Zagotta WN (2006) CNG and HCN channels: two peas, one pod. Annu Rev Physiol 68:375–401. doi:10.1146/annurev.physiol.68.040104.134728

Craven KB, Olivier NB, Zagotta WN (2008) C-terminal movement during gating in cyclic nucleotide-modulated channels. J Biol Chem 283:14728–14738. doi:10.1074/jbc.M710463200

Diller TC, Madhusudan, Xuong NH, Taylor SS (2001) Molecular basis for regulatory subunit diversity in cAMP-dependent protein kinase: crystal structure of the type II beta regulatory subunit. Structure 9:73–82. doi:10.1016/S0969-2126(00)00556-6

Fesenko EE, Kolesnikov SS, Lyubarsky AL (1985) Induction by cyclic GMP of cationic conductance in plasma membrane of retinal rod outer segment. Nature 313:310–313. doi:10.1038/313310a0

Gasteiger J, Marsili M (1980) Iterative partial equalization of orbital electronegativity—a rapid access to atomic charges. Tetrahedron 36:3219–3288. doi:10.1016/0040-4020(80)80168-2

Gordon SE, Varnum MD, Zagotta WN (1997) Direct interaction between amino- and carboxyl-terminal domains of cyclic nucleotide-gated channels. Neuron 19:431–441. doi:10.1016/S0896-6273(00)80951-4

Hay PJ, Wadt WR (1985) Ab initio effective core potentials for molecular calculations. Potentials for the transition metal atoms Sc to Hg. J Chem Phys 82:270–283. doi:10.1063/1.448799

Hofmann F, Biel M, Kaupp UB (2005) International Union of Pharmacology. LI. Nomenclature and structure–function relationships of cyclic nucleotide-regulated channels. Pharmacol Rev 57:455–462. doi:10.1124/pr.57.4.8

Holmgren M, Shin KS, Yellen G (1998) The activation gate of a voltage-gated K^+ channel can be trapped in the open state by an intersubunit metal bridge. Neuron 21:617–621. doi:10.1016/S0896-6273(00)80571-1

Islas LD, Zagotta WN (2006) Short-range molecular rearrangements in ion channels detected by tryptophan quenching of bimane fluorescence. J Gen Physiol 128:337–346. doi:10.1085/jgp.200609556

Kaupp UB, Seifert R (2002) Cyclic nucleotide-gated ion channels. Physiol Rev 82:769–824

Kaupp UB, Niidome T, Tanabe T, Terada S, Bonigk W, Stuhmer W, Cook NJ, Kangawa K, Matsuo H, Hirose T (1989) Primary structure and functional expression from complementary DNA of the rod photoreceptor cyclic GMP-gated channel. Nature 342:762–766. doi:10.1038/342762a0

Körschen HG, Illing M, Seifert R, Sesti F, Williams A, Gotzes S, Colville C, Müller F, Dose A, Godde M (1995) A 240 kDa protein represents the complete beta subunit of the cyclic nucleotide-gated channel from rod photoreceptor. Neuron 15:627–636. doi:10.1016/0896-6273(95)90151-5

Krizek BA, Zawadzke LE, Berg JM (1993) Independence of metal binding between tandem Cys_2His_2 zinc finger domains. Protein Sci 2:1313–1319

Krovetz HS, VanDongen HM, VanDongen AM (1997) Atomic distance estimates from disulfides and high-affinity metal-binding sites in a K^+ channel pore. Biophys J 72:117–126

Kubo Y, Yoshimichi M, Heinemann SH (1998) Probing pore topology and conformational changes of Kir2.1 potassium channels by cysteine scanning mutagenesis. FEBS Lett 435:69–73. doi:10.1016/S0014-5793(98)01038-2

Kurz LL, Zuhlke RD, Zhang HJ, Joho RH (1995) Side-chain accessibilities in the pore of a K^+ channel probed by sulfhydryl-specific reagents after cysteine-scanning mutagenesis. Biophys J 68:900–905

Liu Y, Holmgren M, Jurman ME, Yellen G (1997) Gated access to the pore of a voltage-dependent K+ channel. Neuron 19:175–184. doi:10.1016/S0896-6273(00)80357-8

Loo TW, Clarke DM (2001) Determining the dimensions of the drug-binding domain of human P-glycoprotein using thiol cross-linking compounds as molecular rulers. J Biol Chem 276:36877–36880. doi:10.1074/jbc.C100467200

Loussouarn G, Makhina EN, Rose T, Nichols CG (2000) Structure and dynamics of the pore of inwardly rectifying K_{ATP} channels. J Biol Chem 275:1137–1144. doi:10.1074/jbc.275.2.1137

Matulef K, Flynn GE, Zagotta WN (1999) Molecular rearrangements in the ligand-binding domain of cyclic nucleotide-gated channels. Neuron 24:443–452. doi:10.1016/S0896-6273(00)80857-0

Mazzolini M, Punta M, Torre V (2002) Movement of the C-helix during the gating of cyclic nucleotide-gated channels. Biophys J 83:3283–3295

Mazzolini M, Nair AV, Torre V (2008) A comparison of electrophysiological properties of the CNGA1, $CNGA1_{tandem}$ and $CNGA1_{cys\text{-}free}$ channels. Eur Biophys J 37:947–959. doi:10.1007/s00249-008-0312-1

Menini A (1990) Currents carried by monovalent cations through cyclic GMP-activated channels in excised patches from salamander rods. J Physiol 424:167–185

Molday RS, Molday LL, Dose A, Clark-Lewis I, Illing M, Cook NJ, Eismann E, Kaupp UB (1991) The cGMP-gated channel of the rod photoreceptor cell characterization and orientation of the amino terminus. J Biol Chem 266:21917–21922

Nair AV, Mazzolini M, Codega P, Giorgetti A, Torre V (2006) Locking CNGA1 channels in the open and closed state. Biophys J 90:3599–3607. doi:10.1529/biophysj.105.073346

Nakamura T, Gold GH (1987) A cyclic nucleotide-gated conductance in olfactory receptor cilia. Nature 325:442–444. doi:10.1038/325442a0

Nizzari M, Sesti F, Giraudo MT, Virginio C, Cattaneo A, Torre V (1993) Single-channel properties of cloned cGMP-activated channels from retinal rods. Proc Biol Sci 254:69–74. doi:10.1098/rspb.1993.0128

Passner JM, Schultz SC, Steitz TA (2000) Modeling the cAMP-induced allosteric transition using the crystal structure of CAP-cAMP at 2.1 Å resolution. J Mol Biol 304:847–859. doi:10.1006/jmbi.2000.4231

Pearlman DA, Case DA, Caldwell JW, Ross WS, Cheatham TEIII, DeBolt S, Ferguson D, Seibel G, Kollman P (1995) AMBER, a package of computer programs for applying molecular mechanics, normal mode analysis, molecular dynamics and free energy calculations to simulate the structural and energetic properties of molecules. Comput Phys Commun 91:1–41. doi:10.1016/0010-4655(95)00041-D

Picco C, Menini A (1993) The permeability of the cGMP-activated channel to organic cations in retinal rods of the tiger salamander. J Physiol 460:741–758

Ren X, Nicoll DA, Philipson KD (2006) Helix packing of the cardiac Na^+–Ca^{2+} exchanger: proximity of transmembrane segments 1, 2, and 6. J Biol Chem 281:22808–22814. doi:10.1074/jbc.M604753200

Roncaglia P, Becchetti A (2001) Cyclic-nucleotide-gated channels: pore topology in desensitizing E19A mutants. Pflugers Arch 441:772–780. doi:10.1007/s004240000480

Rosenbaum T, Gordon SE (2002) Dissecting intersubunit contacts in cyclic nucleotide-gated ion channels. Neuron 33:703–713. doi:10.1016/S0896-6273(02)00599-8

Rothberg BS, Shin KS, Yellen G (2003) Movements near the gate of a hyperpolarization-activated cation channel. J Gen Physiol 122:501–510. doi:10.1085/jgp.200308928

Russell RB, Barton GJ (1992) Multiple protein sequence alignment from tertiary structure comparison: assignment of global and residue confidence levels. Proteins 14:309–323. doi:10.1002/prot.340140216

Ryckaert J-P, Ciccotti G, Berendsen HJC (1977) Numerical integration of the Cartesian equations of motion of a system with constraints: molecular dynamics of n-alkanes. J Comput Phys 23:327–341. doi:10.1016/0021-9991(77)90098-5

Šali A, Blundell TL (1993) Comparative protein modelling by satisfaction of spatial restraints. J Mol Biol 234:779–815. doi:10.1006/jmbi.1993.1626

Schuettelkopf AW, van Aalten DMF (2004) PRODRG—a tool for high-throughput crystallography of protein–ligand complexes. Acta Crystallogr D60:1355–1363

Sesti F, Eismann E, Kaupp UB, Nizzari M, Torre V (1995) The multi-ion nature of the cGMP-gated channel from vertebrate rods. J Physiol 487(Pt 1):17–36

Shammat IM, Gordon SE (1999) Stoichiometry and arrangement of subunits in rod cyclic nucleotide-gated channels. Neuron 23:809–819. doi:10.1016/S0896-6273(01)80038-6

Still WC, Tempczyk A, Hawley RC, Hendrickson T (1990) Semianalytical treatment of solvation for molecular mechanics and dynamics. J Am Chem Soc 112:6127–6129. doi:10.1021/ja00172a038

Sun ZP, Akabas MH, Goulding EH, Karlin A, Siegelbaum SA (1996) Exposure of residues in the cyclic nucleotide-gated channel pore: P region structure and function in gating. Neuron 16:141–149. doi:10.1016/S0896-6273(00)80031-8

Thompson JD, Higgins DG, Gibson TJ (1994) CLUSTAL W: improving the sensitivity of progressive multiple sequence alignment through sequence weighting, position-specific gap penalties and weight matrix choice. Nucleic Acids Res 22:4673–4680. doi:10.1093/nar/22.22.4673

Wang J, Wolf RM, Caldwell JW, Kollman PA, Case DA (2004) Development and testing of a general amber force field. J Comput Chem 25:1157–1174. doi:10.1002/jcc.20035

Wu J, Brown S, Xuong NH, Taylor SS (2004a) RIalpha subunit of PKA: a cAMP-free structure reveals a hydrophobic capping mechanism for docking cAMP into site B. Structure 12:1057–1065. doi:10.1016/j.str.2004.03.022

Wu J, Jones JM, Nguyen-Huu X, Ten Eyck LF, Taylor SS (2004b) Crystal structures of RIα subunit of cyclic adenosine 5'-monophosphate (cAMP)-dependent protein kinase complexed with (R_p)-adenosine 3',5'-cyclic monophosphothioate and (S_p)-adenosine 3',5'-cyclic monophosphothioate, the phosphothioate

analogues of cAMP. Biochemistry 43:6620–6629. doi:10.1021/bi0302503

Yellen G, Sodickson D, Chen TY, Jurman ME (1994) An engineered cysteine in the external mouth of a K^+ channel allows inactivation to be modulated by metal binding. Biophys J 66:1068–1075

Zagotta WN, Olivier NB, Black KD, Young EC, Olson R, Gouaux E (2003) Structural basis for modulation and agonist specificity of HCN pacemaker channels. Nature 425:200–205. doi:10.1038/nature01922

Zagotta WN, Siegelbaum SA (1996) Structure and function of cyclic nucleotide-gated channels. Annu Rev Neurosci 19:235–263. doi:10.1146/annurev.ne.19.030196.001315

Zheng J, Trudeau MC, Zagotta WN (2002) Rod cyclic nucleotide-gated channels have a stoichiometry of three CNGA1 subunits and one CNGB1 subunit. Neuron 36:891–896. doi:10.1016/S0896-6273(02)01099-1

Zhong H, Molday LL, Molday RS, Yau KW (2002) The heteromeric cyclic nucleotide-gated channel adopts a 3A:1B stoichiometry. Nature 420:193–198. doi:10.1038/nature01201

Zimmerman AL, Baylor DA (1986) Cyclic GMP-sensitive conductance of retinal rods consists of aqueous pores. Nature 321:70–72. doi:10.1038/321070a0

Zimmerman AL, Yamanaka G, Eckstein F, Baylor DA, Stryer L (1985) Interaction of hydrolysis-resistant analogs of cyclic GMP with the phosphodiesterase and light-sensitive channel of retinal rod outer segments. Proc Natl Acad Sci USA 82:8813–8817. doi:10.1073/pnas.82.24.8813